Published in final edited form as:
Development. 2008 July ; 135(13): 2215–2220. doi:10.1242/dev.019950.

JAWS coordinates chondrogenesis and synovial joint positioning

Michael L. Sohaskey[1,*], **Jane Yu**[1], **Michael A. Diaz**[2], **Anna H. Plaas**[2], and **Richard M. Harland**[1,*]

1 *Division of Genetics, Genomics and Development, Department of Molecular and Cell Biology, Center for Integrative Genomics, University of California, Berkeley, CA 94720, USA*

2 *Departments of Internal Medicine (Rheumatology) & Biochemistry, Rush University Medical Center, 1725 Harrison Street, Chicago, IL 60612, USA*

SUMMARY

Properly positioned synovial joints are crucial to coordinated skeletal movement. Despite their importance for skeletal development and function, the molecular mechanisms underlying joint positioning are not well understood. We show that mice carrying an insertional mutation in a previously uncharacterized gene, which we have named *Jaws* (*Joints abnormal with splitting*), die perinatally with striking skeletal defects including ectopic interphalangeal joints. These ectopic joints develop along the longitudinal axis and persist at birth, suggesting that JAWS is uniquely required for the orientation and consequent positioning of interphalangeal joints within the endochondral skeleton. *Jaws* mutant mice also exhibit severe chondrodysplasia characterized by delayed and disorganized maturation of growth plate chondrocytes, together with impaired chondroitin sulfation and abnormal metabolism of the chondroitin sulfate proteoglycan aggrecan. Our findings identify JAWS as a key regulator of chondrogenesis and synovial joint positioning required for the restriction of joint formation to discrete, stereotyped locations in the embryonic skeleton.

Keywords

chondrogenesis; synovial joints; interzone; Gdf5; chondroitin sulfate; extracellular matrix; mouse embryo

INTRODUCTION

Synovial joints segment the developing cartilage template into individual skeletal elements while providing flexibility and structural stability between these elements. Histologically, the earliest sign of synovial joint formation is the appearance of the interzone (Mitrovic 1977), which occurs at approximately embryonic day (E) 12.5–13.5 in mouse digits. Several signaling pathways are implicated in the molecular specification of the joint interzone, including those downstream of the secreted proteins Growth differentiation factor 5 (Gdf5) and Wnt9a (Hartmann and Tabin, 2001; Pacifici et al., 2005; Khan et al., 2007). In contrast, the molecular mechanisms that control spatial positioning of the joint interzone are not well understood. Here we identify a previously uncharacterized protein, which we have named JAWS (Joints Abnormal With Splitting), as a novel and essential coordinator of cartilage formation and synovial joint positioning.

*Authors for correspondence (e-mail: sohaskey@berkeley.edu, harland@berkeley.edu).

RESULTS AND DISCUSSION

JAWS is required for the development of the endochondral skeleton

Jaws (also known as *Impad1* – Mouse Genome Informatics) was identified in an insertional mutagenesis screen for genes encoding secreted and transmembrane proteins essential for mammalian development (Mitchell et al., 2001). The *Jaws/Impad1* locus encodes a predicted protein of ~39 kDa having an amino-terminal hydrophobic domain and a consensus inositol monophosphatase catalytic motif. Insertion of the gene-trap vector into the third of four introns fuses the first 213 amino acids of the JAWS protein in-frame with a βgeo reporter, resulting in less than 0.2% expression of wild-type (WT) transcripts and negligible expression of the endogenous protein (see Fig. S1 in the supplementary material). Together with the observation that βgeo fusion proteins generated by this “secretory trap” accumulate in cytoplasmic inclusion bodies (Skarnes et al., 1995; Mitchell et al., 2001), these data suggest that the *Jaws* insertion creates a null or strongly hypomorphic allele.

Jaws mRNA and protein expression is widespread during embryogenesis and early postnatal life (Fig. 1A and see Fig. S1 in the supplementary material). In the developing skeleton, X-gal staining demonstrated β-galactosidase activity throughout the cartilage growth plate and in primary ossification centers, with prominent staining in chondrogenic condensations, perichondrium and articular chondrocytes (Fig. 1A and data not shown).

Mice carrying one copy of the *Jaws* insertional mutation ($Jaws^{+/-}$) appeared phenotypically indistinguishable from WT littermates. In contrast, mice homozygous for the insertion ($Jaws^{-/-}$) died perinatally with cleft secondary palate (see Fig. S2 in the supplementary material). $Jaws^{-/-}$ neonates exhibited severe dwarfism with stunted limbs, hypoplastic ribcages, and rounder, shortened craniofacies (Fig. 1B, C). The cranial vault and clavicles, which form without a cartilage intermediate, were largely unaffected (Fig. 1C and data not shown). These results reveal that the skeletal defects in $Jaws^{-/-}$ embryos were restricted to elements formed through endochondral ossification. Defects in chondrogenesis were apparent by E12.5 in $Jaws^{-/-}$ embryos (see Fig. S3 in the supplementary material), despite robust expression of the chondrogenic markers *Sox9*, *Sox5* and *Col2a1* (see Fig. S4 in the supplementary material) (Akiyama et al., 2002). This latter observation suggests that JAWS is dispensable for the formation of prechondrogenic condensations from limb bud mesenchyme.

In the embryonic growth plate, chondrocytes align in a pseudocolumnar arrangement along the longitudinal axis according to their differentiation status, which is reflected in the demarcation of four histologically and molecularly distinct chondrocytic zones: resting, proliferative, prehypertrophic and hypertrophic (Kronenberg, 2003). Histologically, $Jaws^{-/-}$ chondrocytes lacked the pseudocolumnar organization of their WT counterparts (Fig. 1D). Mutant growth plates were hypocellular, with discontinuities in alcian blue staining revealing regions devoid of extracellular matrix (ECM). After E15.5, ectopic chondrocytes were regularly seen impinging on the primary ossification center in $Jaws^{-/-}$ embryos (Fig. 1D, arrow).

JAWS deficiency delays chondrocyte maturation and disrupts long-range Ihh signaling in the growth plate

To analyze growth plate maturation in molecular detail, we examined markers of chondrocyte differentiation by in situ hybridization at E14.5 (Fig. 2A). Expression of the proliferating chondrocyte marker *Col2a1* was largely excluded from the central *Col10a1*-expressing hypertrophic zone in WT long bones, whereas in $Jaws^{-/-}$ embryos *Col2a1* expression partially overlapped this *Col10a1* domain. During hypertrophic differentiation, maturing chondrocytes

abruptly switch from *Col2a1* to *Col10a1* expression; thus, this overlap in the two domains suggests that many *Jaws*$^{-/-}$ chondrocytes were in a delayed intermediate state of already expressing *Col10a1* without yet having downregulated *Col2a1* expression (St-Jacques et al., 1999). Similarly, WT expression of *Ihh* or *Pthr* appeared in symmetrical domains of prehypertrophic chondrocytes flanking the central *Col10a1* domain (Kronenberg, 2003); however, one continuous domain of expression overlapping that of *Col10a1* was seen for each gene in *Jaws*$^{-/-}$ embryos. Altered expression of two downstream targets of Ihh signaling, *Ptch1* and *Pthrp*, was also evident. *Ptch1* expression was unchanged in the perichondrium and proliferating chondrocytes proximal to the Ihh source in *Jaws*$^{-/-}$ embryos; however, expression of *Ptch1* in resting and periarticular chondrocytes was markedly diminished, as was expression of *Pthrp* (Fig. 2A, arrows). This finding implies normal short-range but disrupted long-range Ihh signaling in the *Jaws*$^{-/-}$ growth plate, likely resulting from compromised ECM integrity (see below). Collectively, these data indicate a delay in chondrocyte maturation in *Jaws*$^{-/-}$ embryos. Terminal hypertrophic chondrocyte differentiation was also delayed in E15.5 *Jaws*$^{-/-}$ cartilage, as evidenced by a persistent central domain of *Col10a1* expression and reduced expression of the terminal differentiation markers *Mmp13* and *Osteopontin* (Fig. 2B). Delayed chondrocyte maturation was most conspicuous in the hindlimb, where the knee joint failed to form and where the tibia retained a homogeneous population of small, *Col2a1*-expressing chondrocytes at E18.5 (Fig. 3A and see Fig. S5 in the supplementary material). Finally, expression of the osteoprogenitor markers *Runx2* (Kronenberg, 2003) and *Tcf1* (Glass et al., 2005) was similar in WT and *Jaws*$^{-/-}$ long bones excluding the tibia (Fig. 2A and data not shown), suggesting that subsequent osteogenesis, when it occurred, initiated normally.

Ectopic joints form in the digits of *Jaws*$^{-/-}$ mice

The most striking defect in *Jaws*$^{-/-}$ embryos was seen in the digits, where skeletal preparations revealed longitudinally oriented cavities that lacked Alcian blue staining and were flanked by cartilage (Fig. 3A). These nonchondrogenic cavities, which were first apparent when the WT interzone formed at approximately E13.5, extended from the presumptive metacarpophalangeal/metatarsophalangeal joint to the distalmost phalanx in all digits, appearing discontinuous in forelimbs while bisecting and spanning each hindlimb element. Two main possibilities could explain the occurrence of these cavities: either they result from aberrant cell death, or they represent ectopic joints. To distinguish these possibilities, we first examined the early joint marker *Gdf5* by whole-mount in situ hybridization and found that *Gdf5* expression extended longitudinally throughout these cavities (Fig. 3B and Fig. S6 in the supplementary material). Likewise, expression of all joint markers examined, including *Gli3*, *Wnt9a*, *Sulf1*, *Cutl1*, *Stc1*, *Hip1* and activated β-catenin (Guo et al., 2004;Hill et al., 2005;Pacifici et al., 2005;Mak et al., 2006;Zhao et al., 2006;Khan et al., 2007) overlapped the *Gdf5* expression domain (Fig. 3C and data not shown), suggesting that cells within these cavities exhibited a joint-like fate. Histologically, these cells resembled WT joint progenitors in having a flattened, more mesenchymal appearance than surrounding chondrocytes (Fig. 3C and data not shown). TUNEL analysis demonstrated similar numbers of apoptotic cells in WT and *Jaws*$^{-/-}$ joints at all stages examined (E12.5–E17.5; see Fig. S7 in the supplementary material, and data not shown), further excluding cell death as a disproportionate contributor to the joint phenotype. Likewise, consistent cartilage staining in the digits of E12.5 *Jaws*$^{-/-}$ autopods prior to the appearance of the joint interzone suggested that ectopic joints were not a secondary consequence of diminished ECM formation (see Fig. S3 in the supplementary material, and data not shown). Moreover, no changes in the expression of limb polarity markers were evident earlier in E11.5 or E12.5 *Jaws*$^{-/-}$ embryos (see Fig. S8 in the supplementary material).

If the longitudinal cavities in *Jaws*$^{-/-}$ digits represent joints, then they should not only express joint markers but also exclude markers of neighboring cell types. Indeed, expression of the

chondrogenic markers collagen II, aggrecan, and link protein was excluded from prospective *Jaws*$^{-/-}$ joints (Fig. 3D and data not shown) (Schwartz and Domowicz, 2002). Similarly, expression of *Bmpr1b*, normally restricted to articular surfaces flanking the WT joint interzone at E14.5 (Baur et al., 2000;Yi et al., 2000), was seen in an analogous pattern bordering the longitudinal domain of *Gdf5* expression in *Jaws*$^{-/-}$ digits (Fig. 3D). Thus, joint-like structures in *Jaws*$^{-/-}$ digits do not express chondrogenic markers but do maintain their immediate proximity to *Bmpr1b*-expressing articular chondrocytes. In addition, these joint-like structures did not express markers of hypertrophic chondrocytes (*Col10a1*) or osteoblasts (*Runx2*), while expressing WT levels of the tendon and ligament marker *Scx* (Fig. 3E) (Schweitzer et al., 2001). Collectively, these molecular and histological data establish the longitudinal cavities in *Jaws*$^{-/-}$ digits as ectopic joints. The persistence of ectopic joints in neonatal *Jaws*$^{-/-}$ mice defines JAWS as a crucial, novel regulator of synovial joint orientation and positioning. Because misorientation of the interzone necessarily causes an ectopic joint, we use the terms “orientation” and “positioning” interchangeably here.

Cavitation is the late-stage process culminating in formation of the synovial cavity. Cavitation in E18.5 WT forelimb digits was demonstrated by expression of the hyaluronan (HA) receptor CD44 on articular surfaces (Pitsillides, 1999). In contrast, CD44 immunostaining was largely absent from ectopic *Jaws*$^{-/-}$ joints, despite its presence in more proximal joints (Fig. 3F and data not shown). This result indicates a requirement for JAWS in the timely progression to cavitation leading to a functional synovial joint.

Impaired chondroitin sulfation and aberrant aggrecan metabolism in *Jaws*$^{-/-}$ cartilage

From a mechanistic perspective, several features of the *Jaws*$^{-/-}$ phenotype are consistent with defects in chondroitin sulfation pathways. In particular, misaligned chondrocytes, hypocellularity and ECM discontinuities characterize the growth plates of animals lacking chondroitin-4-sulfotransferase 1 (*C4st1*) or the chondroitin sulfate (CS)- and heparan sulfate (HS)-rich proteoglycan perlecan (Klüppel et al., 2005; Schwartz and Domowicz, 2002). Moreover, mutant mice lacking components of the CS synthesis or transport machinery are chondrodysplastic (Schwartz and Domowicz, 2002). For these reasons, we examined whether CS was spatially or quantitatively altered in *Jaws*$^{-/-}$ embryos. Immunostaining for CS demonstrated highest levels in the perichondrium and articular zones of E14.5 limbs (Fig. 4A and data not shown), with intense, uniform extracellular staining in WT digits. In contrast, a faint punctate pattern was observed in *Jaws*$^{-/-}$ digits, much of which appeared to localize intracellularly (Fig. 4A, insets).

We then used fluorophore-assisted carbohydrate electrophoresis to analyze and quantify glycosaminoglycan content in E14.5 limbs. Consistent with our immunostaining data, significant decreases in the proportions of both chondroitin-4-sulfate (C4S) and chondroitin-6-sulfate (C6S) were evident in *Jaws*$^{-/-}$ limbs, with concomitant increases in unsulfated chondroitin (C0S) (Fig. 4B). Importantly, no change in heparan sulfation was observed (Fig. 4C). Moreover, quantities of total CS (including C0S), HS and HA normalized to wet tissue weight were comparable in WT and *Jaws*$^{-/-}$ limbs (Fig. 4D). The expression of *C4st1*, *Slc26a2* and *Papss2* – key regulators of CS biosynthesis and/or transport – was also unchanged, implying that JAWS does not influence CS levels through transcriptional regulation of these genes (see Fig. S9 in the supplementary material). As described above, this specific diminution of chondroitin sulfation is consistent with the *Jaws*$^{-/-}$ growth plate defects and suggests a molecular mechanism by which JAWS coordinates chondrogenesis and joint positioning. As extracellular HS is important for shaping the Ihh morphogen gradient (Koziel et al., 2004), these data also argue that the disruption of long-range Ihh signaling in the *Jaws*$^{-/-}$ growth plate (Fig. 2A) does not result from a change in HS levels but from a generalized loss of ECM integrity.

Decreased chondroitin sulfation may affect chondrogenesis in part by disrupting the normal metabolism of CS-containing proteoglycans such as aggrecan. Aggrecan is the predominant CS proteoglycan of the cartilage matrix and is critical to normal chondrogenesis and ECM integrity (Schwartz and Domowicz, 2002). The CS chains of aggrecan are essential for its efficient secretion and for binding and proteolytic cleavage by the aggrecanase Adamts4 (Kiani et al., 2001; Tortorella et al., 2000). Therefore, we assessed whether *Jaws*$^{-/-}$ embryos show impaired expression and/or turnover of aggrecan. Aggrecan immunostaining revealed mottled, variable expression throughout E14.5 *Jaws*$^{-/-}$ cartilage, in contrast to the robust, consistent WT staining pattern (Fig. 4E and data not shown). Notably, mRNA and protein levels of two other abundant cartilage ECM proteins, collagen II and link protein, were unchanged, suggesting that abnormal aggrecan expression was not a secondary consequence of delayed chondrocyte maturation (see Fig. S10 in the supplementary material, and data not shown). To confirm and extend this aggrecan result, an antibody (anti-CDAGWL) that recognizes intact aggrecan as well as several well-characterized cleavage products was used to analyze limb protein extracts (Arner, 2002). Under dissociative conditions, markedly reduced amounts of both full-length aggrecan (Fig. 4F, arrow) and carboxy-terminally cleaved aggrecan fragments (Fig. 4F, bracket) were extracted from *Jaws*$^{-/-}$ relative to WT limbs. This reduction was greater in hindlimbs, where more severe chondrogenic and joint defects were noted (Fig. 3A and see Fig. S5 in the supplementary material). As an internal control, successive nondissociative extractions yielded similar levels of a 65-kDa aggrecan fragment that is likely to result from transient expression and rapid cleavage in extracartilaginous tissue (Fig. 4F, arrowhead) (Arner 2002). Collectively, these data suggest that impaired CS sulfation and abnormal aggrecan metabolism contribute to the chondrodysplasia and aberrant joint positioning in *Jaws*$^{-/-}$ embryos.

Although the precise mechanism by which JAWS influences CS sulfation and ECM integrity is unclear, CS sulfation has been reported to modulate cell adhesion and migration (Zou et al., 2004), consistent with the misalignment of both growth plate chondrocytes and the axis of joint formation in *Jaws*$^{-/-}$ embryos. Moreover, the particular importance of CS sulfation for chondrogenesis may explain why mutation of *Jaws*, a widely expressed gene, produces defects that are relatively specific to endochondral ossification.

Importantly, this genetic loss-of-function approach distinguishes our findings from previous demonstrations of ectopic joint formation caused by overexpressing Wnt9a or activated β-catenin in vivo or by blocking α5β1 integrin function in limb explant cultures (Hartmann and Tabin, 2001; Guo et al., 2004; Garciadiego-Cázares et al., 2004). Our findings also contrast with data obtained by inactivation of the hypoxia-inducible factor 1 (*Hif1α*) gene in mouse limb mesenchyme. Conditional deletion of *Hif1α* using *Prx1-Cre* produces longitudinal cavities that are superficially similar to those seen in *Jaws*$^{-/-}$ digits; however, unlike ectopic *Jaws*$^{-/-}$ joints, *Hif1α*-null cavities form prior to the WT joint interzone and do not express joint markers such as *Wnt9a* and *Bmp2* (Amarilio et al., 2007; Provot et al., 2007). *Gdf5* is expressed primarily in diffuse transverse (rather than longitudinal) stripes in *Hif1α*-null digits, leading Provot and colleagues to conclude that after an initial developmental delay, synovial joints of normal appearance do form in the digits of these mice. Together, data presented by both groups argue that the *Hif1α*-null digit phenotype reflects delayed joint specification caused by aberrant differentiation of hypoxic chondrocytes.

By demonstrating the persistence of ectopic joints in *Jaws*$^{-/-}$ digits, our studies identify JAWS as a novel regulator in the establishment of the interphalangeal joint axes. Because cells in the ectopic *Jaws*$^{-/-}$ joint express appropriate early interzone markers (Fig. 3B, C), we conclude that the molecular specification and the spatial positioning of the synovial joint interzone are genetically separable processes. Similarly, the restriction of ectopic joints to digits and the lack of knee joints in *Jaws*$^{-/-}$ embryos support the notion that distinct *Jaws*-dependent mechanisms

govern synovial joint development at different sites in the embryonic skeleton. Overall, *Jaws*$^{-/-}$ mice provide a unique animal model for exploring the tightly coordinated processes of chondrogenesis and joint morphogenesis and for better understanding the etiology of joint degeneration leading to debilitating diseases such as osteoarthritis.

MATERIALS AND METHODS

Animals

The KST245 mouse embryonic stem cell line, containing an insertion of the pGT1TMpfs gene trap vector in the *Jaws/Impad1* locus, was isolated and characterized as described (Mitchell et al., 2001). *Jaws* F1 heterozygotes were backcrossed to C57BL/6 mice for six generations before intercrossing. Genotyping was performed by X-gal staining of yolk sacs and/or tail biopsies, or by RT-PCR using primers flanking the insertion site (sequences available upon request).

Expression studies

Jaws transcripts were detected by Northern blotting of Trizol-extracted total RNA, probed with a cDNA fragment spanning nucleotides 726–1158 of the *Jaws* mRNA (GenBank accession number BC145952). Alternatively, *Jaws* expression was assessed by quantitative RT-PCR using SYBR Green reagents (Applied Biosystems). For immunoblotting of E13.5 embryo lysates (60 μg), a polyclonal antiserum was raised against the peptide epitope N-CRESNVLHEKSKGKTREGADD-C corresponding to residues 83–102 of the JAWS protein.

Histology, in situ hybridization and immunohistochemistry

Alcian blue and alizarin red staining of skeletal preparations and histological sections, X-gal staining of embryos, and in situ hybridization were performed as described (Nagy, 2003). To enhance contrast against the Hoechst counterstain, the radioactive ISH images were photographed in bright-field and then pseudo-colored red using the “Colorize” option within the “Hue/Saturation” command in Adobe Photoshop 7.0. Immunohistochemistry on paraffin sections was carried out after antigen retrieval, using Alexa Fluor-conjugated secondary antibodies and the following primary antibodies: mouse aggrecan 12/21/1-C-6 and link protein 9/30/8-A-4 (Developmental Studies Hybridoma Bank), mouse β-catenin (BD Biosciences), mouse chondroitin sulfate CS-56 (Sigma-Aldrich), rabbit collagen II (Abcam), and rat CD44S (Chemicon). Apoptotic cells were labeled using the In Situ Cell Death Detection kit (Roche).

Fluorophore-assisted carbohydrate electrophoresis (FACE)

The composition and amount of chondroitin sulfate and heparan sulfate were analyzed as described (Plaas et al., 2001; Gao et al., 2004). Values for total CS, HS and HA were normalized to wet tissue weight. FACE data were analyzed by a two-tailed Student’s *t*-test, and values were considered statistically significant at $P < 0.05$.

Protein extraction and aggrecan immunoblotting

Successive nondissociative extractions (0.15 M NaCl, then 0.15 M NaCl + 0.5% CHAPS) of E14.5 limb tissue were followed by one dissociative extraction (4 M guanidinium HCl + 0.5% CHAPS) to solubilize matrix-associated proteins. Loadings for SDS-PAGE were normalized to wet tissue weight, and immunoblots were processed with polyclonal CDAGWL antibodies directed against the amino-terminal G1 domain of aggrecan. Blots were exposed to film simultaneously and developed identically.

Supplementary Material

Refer to Web version on PubMed Central for supplementary material.

Acknowledgements

We thank Jen-Yi Lee, David Stafford, Danielle Behonick and Pete Savage for critical reading of the manuscript; Edivinia Pangilinan for mouse husbandry; Lisa Brunet for technical expertise and the *Cutl1* in situ hybridization probe; and Céline Colnot for instruction on in situ hybridization and the *Mmp13* and *Osteopontin* probes. We thank B. de Crombrugghe, M. Hilton and F. Long, S. Dymecki, A. McMahon, Y. Yang, G. Karsenty, P.-T. Chuang, G. DiMattia, R. Johnson, D. Kingsley, G. Martin, and M. Scott for in situ hybridization probes. Monoclonal antibodies 12/21/1-C-6 and 9/30/8-A-4 developed by B. Caterson were obtained from the Developmental Studies Hybridoma Bank developed under the auspices of the NICHD and maintained by The University of Iowa, Department of Biological Sciences, Iowa City, IA 52242. This work was supported by a grant from the NIH (R.M.H.). M.L.S. was a Michael Geisman Fellow of the Osteogenesis Imperfecta Foundation, and a Foundation for Advanced Cancer Studies and Merck Fellow of the Life Sciences Research Foundation.

References

Akiyama H, Chaboissier MC, Martin JF, Schedl A, de Crombrugghe B. The transcription factor Sox9 has essential roles in successive steps of the chondrocyte differentiation pathway and is required for expression of Sox5 and Sox6. Genes Dev 2002;16:2813–28. [PubMed: 12414734]

Amarilio R, Viukov SV, Sharir A, Eshkar-Oren I, Johnson RS, Zelzer E. HIF1α regulation of Sox9 is necessary to maintain differentiation of hypoxic prechondrogenic cells during early skeletogenesis. Development 2007;134:3917–28. [PubMed: 17913788]

Arner EC. Aggrecanase-mediated cartilage degradation. Curr Opin Pharmacol 2002;2:322–9. [PubMed: 12020478]

Baur ST, Mai JJ, Dymecki SM. Combinatorial signaling through BMP receptor IB and GDF5: shaping of the distal mouse limb and the genetics of distal limb diversity. Development 2000;127:605–19. [PubMed: 10631181]

Gao G, Plaas A, Thompson VP, Jin S, Zuo F, Sandy JD. ADAMTS4 (aggrecanase-1) activation on the cell surface involves C-terminal cleavage by glycosylphosphatidyl inositol-anchored membrane type 4-matrix metalloproteinase and binding of the activated proteinase to chondroitin sulfate and heparan sulfate on syndecan-1. J Biol Chem 2004;279:10042–51. [PubMed: 14701864]

Garciadiego-Cazares D, Rosales C, Katoh M, Chimal-Monroy J. Coordination of chondrocyte differentiation and joint formation by α5β1 integrin in the developing appendicular skeleton. Development 2004;131:4735–42. [PubMed: 15329344]

Glass DA 2nd, Bialek P, Ahn JD, Starbuck M, Patel MS, Clevers H, Taketo MM, Long F, McMahon AP, Lang RA, et al. Canonical Wnt signaling in differentiated osteoblasts controls osteoclast differentiation. Dev Cell 2005;8:751–64. [PubMed: 15866165]

Guo X, Day TF, Jiang X, Garrett-Beal L, Topol L, Yang Y. Wnt/β-catenin signaling is sufficient and necessary for synovial joint formation. Genes Dev 2004;18:2404–17. [PubMed: 15371327]

Hartmann C, Tabin CJ. Wnt-14 plays a pivotal role in inducing synovial joint formation in the developing appendicular skeleton. Cell 2001;104:341–51. [PubMed: 11239392]

Hill TP, Spater D, Taketo MM, Birchmeier W, Hartmann C. Canonical Wnt/beta-catenin signaling prevents osteoblasts from differentiating into chondrocytes. Dev Cell 2005;8:727–38. [PubMed: 15866163]

Khan IM, Redman SN, Williams R, Dowthwaite GP, Oldfield SF, Archer CW. The development of synovial joints. Curr Top Dev Biol 2007;79:1–36. [PubMed: 17498545]

Kiani C, Lee V, Cao L, Chen L, Wu Y, Zhang Y, Adams ME, Yang BB. Roles of aggrecan domains in biosynthesis, modification by glycosaminoglycans and product secretion. Biochem J 2001;354:199–207. [PubMed: 11171095]

Kluppel M, Wight TN, Chan C, Hinek A, Wrana JL. Maintenance of chondroitin sulfation balance by chondroitin-4-sulfotransferase 1 is required for chondrocyte development and growth factor signaling during cartilage morphogenesis. Development 2005;132:3989–4003. [PubMed: 16079159]

Koziel L, Kunath M, Kelly OG, Vortkamp A. Ext1-dependent heparan sulfate regulates the range of Ihh signaling during endochondral ossification. Dev Cell 2004;6:801–13. [PubMed: 15177029]

Kronenberg HM. Developmental regulation of the growth plate. Nature 2003;423:332–6. [PubMed: 12748651]

Mak KK, Chen MH, Day TF, Chuang PT, Yang Y. Wnt/beta-catenin signaling interacts differentially with Ihh signaling in controlling endochondral bone and synovial joint formation. Development 2006;133:3695–707. [PubMed: 16936073]

Mitchell KJ, Pinson KI, Kelly OG, Brennan J, Zupicich J, Scherz P, Leighton PA, Goodrich LV, Lu X, Avery BJ, et al. Functional analysis of secreted and transmembrane proteins critical to mouse development. Nat Genet 2001;28:241–9. [PubMed: 11431694]

Mitrovic DR. Development of the metatarsophalangeal joint of the chick embryo: morphological, ultrastructural and histochemical studies. Am J Anat 1977;150:333–47. [PubMed: 920633]

Nagy, A. Manipulating the mouse embryo: a laboratory manual. Cold Spring Harbor, NY: Cold Spring Harbor Laboratory Press; 2003.

Pacifici M, Koyama E, Iwamoto M. Mechanisms of synovial joint and articular cartilage formation: recent advances, but many lingering mysteries. Birth Defects Res C Embryo Today 2005;75:237–48. [PubMed: 16187328]

Pitsillides, AA. The Role of Hyaluronan in Joint Cavitation. In: Archer, CW.; Caterson, B.; Benjamin, M.; Ralphs, JR., editors. Biology of the Synovial Joint. London: Informa Healthcare; 1999. p. 41-62.

Plaas AH, West L, Midura RJ, Hascall VC. Disaccharide composition of hyaluronan and chondroitin/dermatan sulfate. Analysis with fluorophore-assisted carbohydrate electrophoresis. Methods Mol Biol 2001;171:117–28. [PubMed: 11450222]

Provot S, Zinyk D, Gunes Y, Kathri R, Le Q, Kronenberg HM, Johnson RS, Longaker MT, Giaccia AJ, Schipani E. Hif-1α regulates differentiation of limb bud mesenchyme and joint development. J Cell Biol 2007;177:451–64. [PubMed: 17470636]

Schwartz NB, Domowicz M. Chondrodysplasias due to proteoglycan defects. Glycobiology 2002;12:57R–68R.

Schweitzer R, Chyung JH, Murtaugh LC, Brent AE, Rosen V, Olson EN, Lassar A, Tabin CJ. Analysis of the tendon cell fate using Scleraxis, a specific marker for tendons and ligaments. Development 2001;128:3855–66. [PubMed: 11585810]

Skarnes WC, Moss JE, Hurtley SM, Beddington RS. Capturing genes encoding membrane and secreted proteins important for mouse development. Proc Natl Acad Sci U S A 1995;92:6592–6. [PubMed: 7604039]

St-Jacques B, Hammerschmidt M, McMahon AP. Indian hedgehog signaling regulates proliferation and differentiation of chondrocytes and is essential for bone formation. Genes Dev 1999;13:2072–86. [PubMed: 10465785]

Tortorella M, Pratta M, Liu RQ, Abbaszade I, Ross H, Burn T, Arner E. The thrombospondin motif of aggrecanase-1 (ADAMTS-4) is critical for aggrecan substrate recognition and cleavage. J Biol Chem 2000;275:25791–7. [PubMed: 10827174]

Yi SE, Daluiski A, Pederson R, Rosen V, Lyons KM. The type I BMP receptor BMPRIB is required for chondrogenesis in the mouse limb. Development 2000;127:621–30. [PubMed: 10631182]

Zhao W, Sala-Newby GB, Dhoot GK. Sulf1 expression pattern and its role in cartilage and joint development. Dev Dyn 2006;235:3327–35. [PubMed: 17061267]

Zou XH, Foong WC, Cao T, Bay BH, Ouyang HW, Yip GW. Chondroitin sulfate in palatal wound healing. J Dent Res 2004;83:880–5. [PubMed: 15505240]

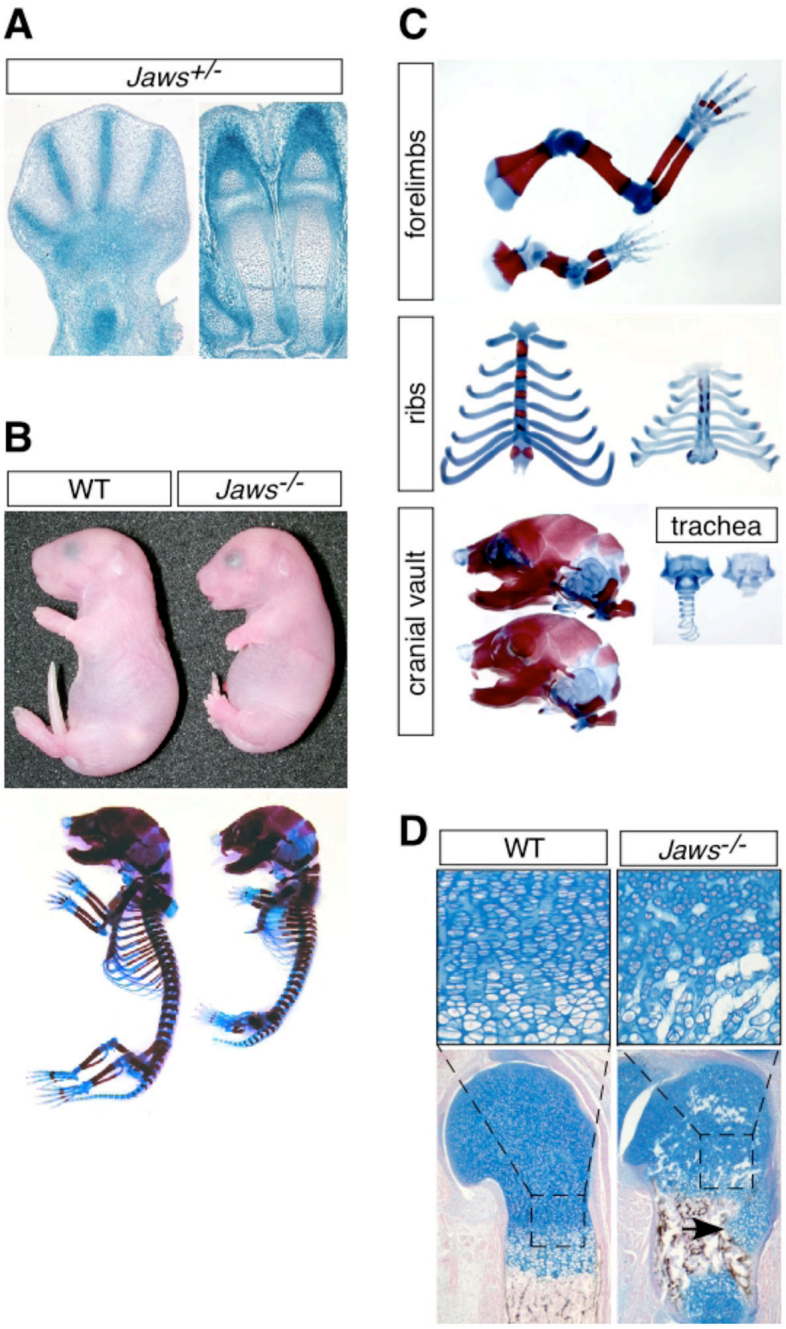

Fig. 1. Insertional mutagenesis of *Jaws* causes chondrodysplasia

(**A**) Widespread β-galactosidase staining from the gene trap reporter in *Jaws*$^{+/-}$ E12.5 forelimb (left) and E15.5 digits (right).

(**B**) Gross morphology (top) and cleared skeletal preparations (bottom) of WT and *Jaws*$^{-/-}$ embryos (E18.5).

(**C**) Skeletal preparations from WT (top or left) and *Jaws*$^{-/-}$ (bottom or right) embryos, showing severe malformation of endochondral elements.

(**D**) Alcian blue/von Kossa staining of humerus sections (E17.5). The arrow indicates ectopic chondrocytes encroaching upon the primary ossification center. Higher-magnification views (top) show hypocellularity and ECM discontinuity in the *Jaws*$^{-/-}$ growth plate.

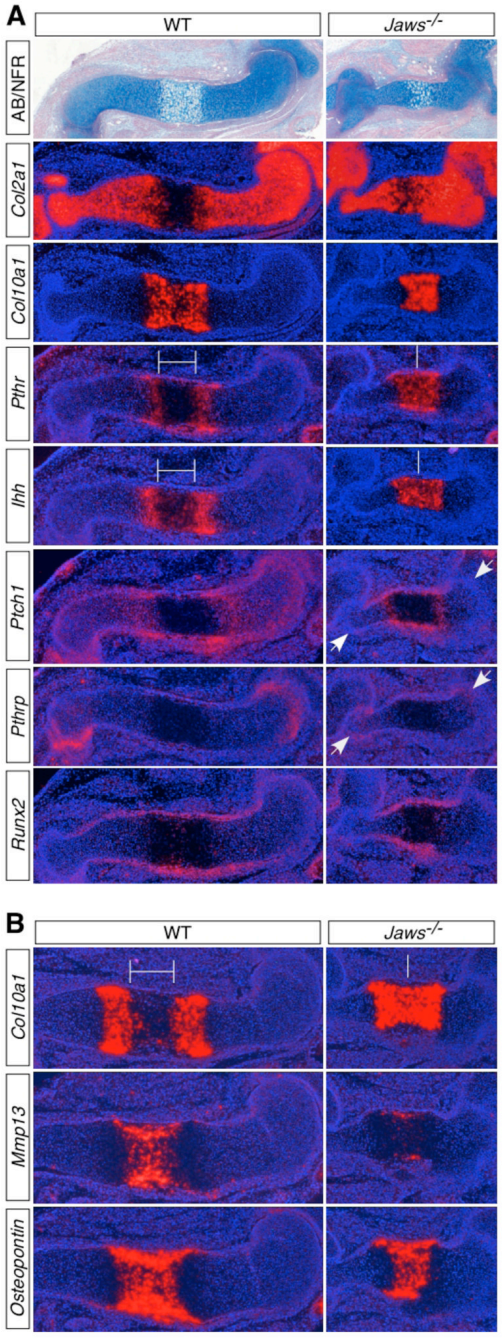

Fig. 2.

Jaws$^{-/-}$ embryos exhibit delayed chondrocyte maturation.

(**A**) Histological and radioactive in situ hybridization (RISH) analysis of chondrocyte maturation in the humerus (E14.5). Top panels show sections stained with Alcian blue and nuclear fast red (AB/NFR). White brackets delineate the separation of WT prehypertrophic zones, which remain continuous in the *Jaws*$^{-/-}$ embryo. Arrows indicate reduced *Ptch1* and *Pthrp* signals in periarticular chondrocytes.

(**B**) RISH analysis showing delayed terminal hypertrophic chondrocyte differentiation in the *Jaws*$^{-/-}$ humerus (E15.5), evidenced by decreased expression of *Mmp13* and *Osteopontin*.

White brackets delineate the separation of WT *Col10a1*-positive hypertrophic zones, which remain continuous in the *Jaws*$^{-/-}$ embryo.

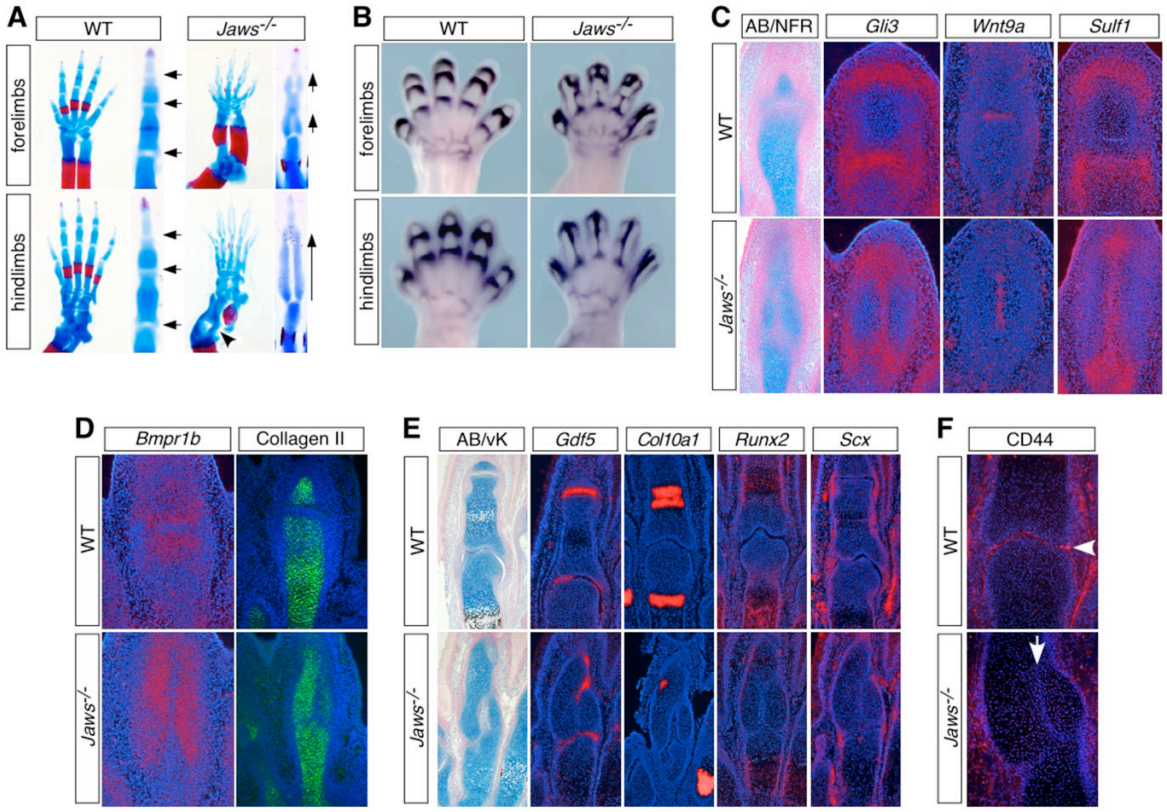

Fig. 3.

Jaws$^{-/-}$ digits develop ectopic joints.

(**A**) Longitudinal cavities lacking alcian blue staining form in *Jaws*$^{-/-}$ digits (E18.5). Higher-magnification views of digit 3 are shown to the right of each limb, with arrows indicating joint position and orientation. The arrowhead indicates failed knee joint formation proximal to a lack of tibial ossification in the *Jaws*$^{-/-}$ hindlimb.

(**B**) Whole-mount ISH for *Gdf5* expression (E14.5).

(**C**) Histological and RISH analysis showing longitudinal expression of joint interzone markers in individual *Jaws*$^{-/-}$ hindlimb digits (E14.5).

(**D**) Exclusion of *Bmpr1b* RNA and Collagen II protein expression from ectopic *Jaws*$^{-/-}$ joints (E14.5).

(**E**) Ectopic joints express *Gdf5* but not markers of hypertrophic chondrocytes (*Col10a1*), osteoblasts (*Runx2*), or tendons and ligaments (*Scx*) (E18.5 forelimb digits). AB/vK, Alcian blue/von Kossa.

(**F**) Defective cavitation of E18.5 ectopic joint (arrow), evidenced by the absence of CD44 immunostaining (arrowhead, WT staining).

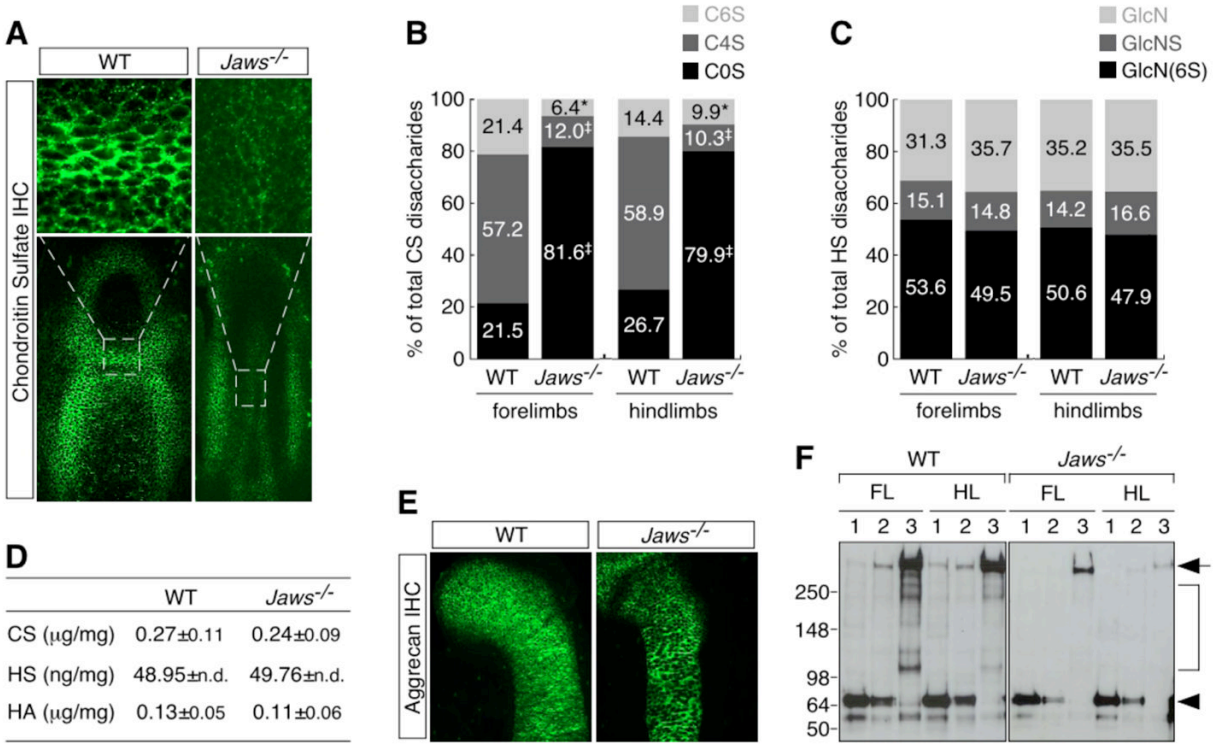

Fig. 4. Impaired chondroitin sulfation and altered aggrecan metabolism in *Jaws*$^{-/-}$ limbs

(**A**) CS immunostaining in hindlimb digits (E14.5). Higher-magnification views (top) reveal sparse, irregular staining in the *Jaws*$^{-/-}$ joint.

(**B,C**) Fluorophore-assisted carbohydrate electrophoresis analysis of chondroitin sulfate (B) and heparan sulfate (C) in E14.5 limbs. The relative proportions and percentages of disaccharides generated with the glycosaminoglycan-specific lysases are shown. For HS, no disaccharides containing 2-sulfated uronic acid (UA) or N,6-sulfated GlcN were detected. galNAc, N-acetylgalactosamine; C0S, ΔUA-galNAc; C4S, ΔUA-galNAc4S; C6S, ΔUA-galNAc6S; glcNAc, N-acetylglucosamine; GlcN, ΔUA-glcNAc; GlcNS, ΔUA-glcNS; GlcN (6S), ΔUA-glcNAc6S. *, $P < 0.025$; ‡, $P < 0.0001$, *Jaws*$^{-/-}$ vs. WT percentage ($n = 5$ pairs per genotype).

(**D**) Comparable amounts (mean and s.d.) of total glycosaminoglycans in WT and *Jaws*$^{-/-}$ hindlimbs, normalized to wet tissue weight. Similar results were obtained for forelimbs. n.d., not determined.

(**E**) Aggrecan immunostaining in the proximal end of the humerus (E14.5).

(**F**) Anti-CDAGWL immunoblots of E14.5 limb protein extracts, showing less full-length aggrecan (arrow, ~350 kDa) and fewer aggrecan cleavage fragments (bracket) in *Jaws*$^{-/-}$ cartilage. Successive nondissociative extractions (lanes 1 and 2; arrowhead indicates a 65-kDa proteolytic fragment) were followed by one dissociative extraction (lane 3).